Current Trends in Technology and Science
ISSN: 2279-0535, Volume: VII, Issue: I

Single Photoionization of Barium (Ba)

Santosh Kumar
Research Scholar, Department of Physics, B. R.A. Bihar University, Muzaffarpur-842001,
sksrivastava0007@gmail.com

D. D. Singh
Assistant Professor, Department of Physics, Motihari Engineering College, Motihari, A. K. University, Patna,
dharm_mit@rediffmail.com

R.P. K Ray
Assistant Professor cum Junior Scientist, Department of Physics, F. B. S. & H., Dr. Rajendra Prasad Central
Agriculture University, Pusa, Samastipur-848125, Bihar, India,
rpkray3@gmail.com

Rajesh Kumar
Assistant Professor, Department of Physics, Sitamarhi Institute of Technology, Sitamarhi, Aryabhatt Knowledge
University Patna, India , rajesh3muz@yahoo.com

Shankar Kumar Choudhary
Research Scholar, Department of Physics, B. R.A. Bihar University, Muzaffarpur-842001, shankarmbd@gmail.com

Abstract — *we have calculated photoionization cross section of Barium (Ba) from 5s state in photon energy range 140 –270 eV in the context of experimental data and theoretical results. We are using time-dependent response method within density functional theory. The present result is encouraging and close to the experimental result.*

Keyword — Atom, cross section, photoionization, Photon.

1. INTRODUCTION

Accurate calculation of photoionization cross-sections of atoms and ions are useful in a variety of investigations in plasma physics and atomic physics. It is particularly useful in the context of flash lamp photo pumping schemes for x-ray lasers. Most of the existing calculations of photoionization cross-sections were done using the single electron or the independent particle model (IPM). In this model, the energy-levels, and wave functions of the atom or ion are first calculated using the Hartree-Fock (HF) method. The interaction of the incident electromagnetic radiation with the atom (or ion) is treated via the first order perturbation theory. Comparison of experimental data with the IPM calculations shows that for some simple systems such as a neutral few electron atom, there is qualitative and sometimes quantitative agreement. However, for many electron atoms and ions with a large number of bound electrons, substantial discrepancies are found between experimental and IPM-data [1]. In our present work, we used the time-dependent linear response approximation within the framework of the relativistic density functional method (DFM) [2, 3, 4] to treat the problem of photoionization. This method incorporates certain advantages over the HF-method. The HF-method is non-local and computationally very elaborate, whereas in the density functional method, one deals with a set of local equations only. This leads to computational simplicity. On the other hand, it is well known from extensive application of the density functional method, that fairly accurate atomic energy levels, wave functions, etc. are obtained. The computational simplicity is even more apparent in the case of relativistic DFM verses relativistic HF-methods. In the DFM, correlation effects of the bound electrons in the atom are accounted for in a simple way via the correlation potential. The Hartree-Fock method, on the other hand, does not take into account electron correlation, although it accounts for non-local exchange effects appropriately. The independent particle method does not take into account the polarization effect of the atom brought about by the incident time-varying radiation field. In the linear response method within the density functional method, this is treated adequately – as will be seen from comparison with the experimental data. In most experimental situations, the incident radiation (from synchrotron sources or lasers) has field strengths small compared to the atomic field strengths. For those experimental conditions, the present model based on linear response is adequate and useful. Calculations of photoionization and photo excitation cross-sections and rates have a number of applications. For the photo pumping scheme for x-ray lasers, these processes play a crucial role in contributing to a population inversion of excited ionic levels. As another example, computation of opacities of plasmas for diagnostic and target response effects require these data as input. In order to model the radiation spectra from hot plasma (via detailed configuration rate equation technique, for example), the photoionization and photo excitation data are required in addition to other bound-bound, bound-free and free-free processes. Accurate calculations are also necessary for interpreting experimentally available data on cross sections. In view of these different applications, there is a need for relativistic modeling of these processes in order to generate accurate data over a wide range of photon energy for a variety of atoms and ions.

2. THEORY

The first part of the calculation is to generate the energy-level spectrum and the wave functions of the particular atom or ion of specific configuration. This is done by using the local density functional method. In order to treat many-electron atoms (with high Z) appropriately, relativistic DFM equations were used. In this method, the following set of equations was solved self-consistently:

$$\left[c\boldsymbol{\alpha}.\mathbf{p}+c^2\beta + u(\mathbf{r})\right]\psi_i(\mathbf{r}) = E_i\,\psi_i(\mathbf{r}) \qquad (1)$$

$$u(\mathbf{r}) = -\frac{Z}{r} + \int\frac{\rho(\mathbf{r}')\,dr'}{|\mathbf{r}-\mathbf{r}'|} + \frac{\partial}{\partial\rho(\mathbf{r})}\left[\rho(\mathbf{r})\,\varepsilon_{XC}\,(\rho(\mathbf{r}))\right] \qquad (2)$$

and $$\rho(\mathbf{r}) = \sum_i f_i\left|\psi_i(\mathbf{r})\right|^2 \qquad (3)$$

In the above, $\rho(\mathbf{r})$ is the electronic charge density of the atom, $\boldsymbol{\alpha}$ and $\boldsymbol{\beta}$ are the Dirac matrices, f_i's are the integral occupation factors corresponding to the number of electrons in each state $\psi_i(\mathbf{r})$ with corresponding energy eigenvalue E_i.The atomic potential $u(\mathbf{r})$ contains, in addition to the nuclear and the electrostatic Hartree term, a contribution arising from the electron exchange and correlation effects. Let us note that the use of integer occupation factors f_i's for the given configuration distinguishes this model from the "average atom model" where the occupation factors are taken to be those given by the statistical Fermi distribution function. The orbital functions are four-component spinors. They are split into major and minor components:

$$\psi(\mathbf{r}) = \begin{pmatrix}\psi^1(\mathbf{r})\\ \psi^2(\mathbf{r})\end{pmatrix} = \begin{pmatrix}(A(r)/r)\; i^l\;\Omega_{jlm}(\mathbf{r})\\ (B(r)/r)\; i^l\;\Omega_{jl'm}(\mathbf{r})\end{pmatrix} \qquad (4)$$

where A and B are major and minor components of the radial functions and $\Omega_{jlm}(\mathbf{r})$ and $\Omega_{jl'm}(\mathbf{r})$ are two-component Pauli spinors with the indicated numbers. The various quantum numbers are related by

$$l' = l + s\,, \qquad j' = l + 1/2, \quad s = l' - 1/2s\,,$$
$$K = -s(j + 1/2); \qquad s = \pm 1 \qquad (5)$$

The differential equations for A and B (in matrix form) are:

$$\frac{d}{dr}\begin{pmatrix}A\\ B\end{pmatrix} = \begin{pmatrix}-K/r & \left(u-E-c^2\right)/cs\\ -\left(u-E+c^2\right)/cs & K/r\end{pmatrix}\begin{pmatrix}A\\ B\end{pmatrix} \qquad (6)$$

In equation (2), ε_{XC} is the exchange-correlation energy of the electrons. In actual calculation, Gunnarsson-Lundquist (G-L) form [3] for exchange-correlation energy and potential was used. It is well known that reliable atomic data is obtained from the use of G-L exchange-correlation. Equation (1)-(6) are solved numerically to self-consistency to obtain the wave functions ψ_i's, the binding energies of each orbital E_i, the atomic charge density $\rho(\mathbf{r})$ and the self-consistent potential $u(\mathbf{r})$. Now consider the effect of an incident time-varying radiation field $E(t) = E_0 e^{i\omega t}$ on the atom. It induces a time-dependent atomic density deviation, $\delta\rho(\mathbf{r},\mathrm{t})$, causing a time-dependent polarization effect. For the linear response method used here, it is convenient to work with the Fourier transform:

$$\delta\rho(\mathbf{r},\mathrm{t}) = \frac{1}{2\pi}\int_{-\infty}^{\infty}\delta\rho(\mathbf{r},\omega)\,e^{-i\omega t}\,d\omega \qquad (7)$$

The net induced density due to the external plus the induced potential is

$$\delta\rho_{ind}(\mathbf{r},\omega) = \int\chi(\mathbf{r},\mathbf{r}',\omega)\left[V_{ext}(\mathbf{r},\omega)+V_{ind}(\mathbf{r},\omega)\right]d\mathbf{r}' \qquad (8)$$

where the induced potential is given by

$$V_{ind}(\mathbf{r},\omega) = \int\frac{\delta\rho(\mathbf{r}',\omega)}{\mathbf{r}-\mathbf{r}'}\,d\mathbf{r}' + \frac{\partial V_{XC}(\rho(\mathbf{r}))}{\partial\rho(\mathbf{r})}\,\delta\rho(\mathbf{r},\omega) \qquad (9)$$

The response function is given by

$$\begin{aligned}\chi(\mathbf{r},\mathbf{r}',\omega) = {} & \sum_i f_i\psi_i^*(\mathbf{r})\,\psi_i(\mathbf{r}')\,\mathrm{G}(\mathbf{r},\mathbf{r}',E_i+\omega)\\ & + \sum_i f_i\psi_i(\mathbf{r})\,\psi_i^*(\mathbf{r}')\,\mathrm{G}^*(\mathbf{r},\mathbf{r}',E_i-\omega)\end{aligned} \qquad (10)$$

and thus involves the wave functions and energy levels of the atoms. The Green's functions are solutions of the inhomogeneous Dirac equation

$$\left[c\boldsymbol{\alpha}.\boldsymbol{\rho}+c^2\beta + u(\mathbf{r}) - E\right]\mathrm{G}(\mathbf{r},\mathbf{r}',E) = -\delta(\mathbf{r}-\mathbf{r}') \qquad (11)$$

In actual calculation, angular decomposition of the Green's function in terms of spherical harmonics is done and the radial part is treated separately as follows: The Green's function G in equation (11) has 16 components, which are represented in matrix form

$$G(\mathbf{r},\mathbf{r}',E) = \begin{pmatrix}G^{11}(\mathbf{r},\mathbf{r}'|E) & G^{12}(\mathbf{r},\mathbf{r}'|E)\\ G^{21}(\mathbf{r},\mathbf{r}'|E) & G^{22}(\mathbf{r},\mathbf{r}'|E)\end{pmatrix}$$

The angular decomposition of various terms are

$$G^{11}(\mathbf{r},\mathbf{r}'|E) = \sum_{jlm}\Omega_{jlm}(\mathbf{r})\,G_{jl}^{11}(\mathbf{r},\mathbf{r}'|E)\,\Omega_{jlm}^{N}(\mathbf{r}')$$
$$G^{12}(\mathbf{r},\mathbf{r}'|E) = \sum_{jlm} i^{l-l'}\Omega_{jlm}(\mathbf{r})\,G_{jl}^{12}(\mathbf{r},\mathbf{r}',|E)\,\Omega_{jlm}^{*}(\mathbf{r}')$$
$$G^{21}(\mathbf{r},\mathbf{r}'|E) = \sum_{jlm} i^{l'-l}\Omega_{jl'm}(\mathbf{r})\,G_{jl}^{21}(\mathbf{r},\mathbf{r}',|E)\,\Omega_{jlm}^{*}(\mathbf{r}')$$
$$G^{22}(\mathbf{r},\mathbf{r}'|E) = \sum_{jl'm}\Omega_{jl'm}(\mathbf{r})\,G_{jl'}^{22}(\mathbf{r},\mathbf{r}',|E)\,\Omega_{jl'm}^{*}(\mathbf{r}') \qquad (12)$$

The radial part $G^{\alpha\beta}(\mathbf{r},\mathbf{r}'|E)$ are solutions of the radial inhomogeneous Dirac equation

$$G_{jl}^{\alpha\beta}(\mathbf{r},\mathbf{r}'|E) = \begin{cases}\mathrm{v}_{jl}^{\alpha}(r)\mathrm{v}_{jl}^{\beta}(r')/(rr'W_{jl}) & r < r'\\ \mathrm{v}_{jl}^{\alpha}(r)\mathrm{v}_{jl}^{\beta}(r')/(rr'W_{jl}) & r > r'\end{cases} \qquad (13)$$

W_{jl} is the Wronskian

$$W_{jl} = eS_{jl}\left[\mathrm{v}_{jl}^2(r)\,\bar{\mathrm{v}}_{jl}^1(r) - \bar{\mathrm{v}}_{jl}^2(r)\,\mathrm{v}_{jl}^1(r)\right] = \text{const.}$$

$\bar{v}^1_{jl}(r)$ and $\bar{v}^2_{jl}(r)$ are major and minor component radial functions that are real and regular at r = 0. $\bar{v}^1_{jl}(r)$ and $\bar{v}^2_{jl}(r)$ major and minor comment radial functions which (for E > c^2) are complex and obey outgoing wave boundary conditions at r = ∞. The phase for $\bar{v}^1_{jl}$ and $\bar{v}^2_{jl}$ are real and decay exponentially at large radii.

With the above representations, the polarizability $\chi(\mathbf{r},\mathbf{r}',\omega)$ is given by

$$\chi_j(\mathbf{r},\mathbf{r}',\omega)=\sum f_i(2j_2+1)(2l_1+1)(2l_2+1)$$

$$\left[\begin{pmatrix} l_1 & l_2 & \bar{l} \\ 0 & 0 & 0 \end{pmatrix}\begin{pmatrix} \bar{l} & l_1 & l_2 \\ 1/2 & j_2 & j_1 \end{pmatrix}\right]^2$$

$$\frac{1}{W_{j_2 l_2}(E_i \pm \omega)}$$

$$\left[A_i(r)\, v^1_{j_2 l_2}(r|\varepsilon_i \pm \omega) \pm i^{S_1 - S_2} B_i(r)\, v^2_{j_2 l_2}(r|\varepsilon_i \pm \omega)\right]$$

$$\left[A_i(r')\, \bar{v}^1_{j_2 l_2}(r'|\varepsilon_i \pm \omega) \pm i^{S_2 - S_1} B_i(r')\, \bar{v}^2_{j_2 l_2} \quad (14)\right.$$

$$\left.(r'|\varepsilon_i \pm \omega)/(rr')^2 \,\Big|\,\right]$$

when $r < r'$, and r and r' are interchanged on the right side of equation (14) when $r > r'$. The index i stands for the quantum numbers (n, l_1, j_1, s_1,) of a bound state and f_i fore the occupation factors. The summation is over all indices except I and over both + ω and – ω. For the case of –ω, the complex conjugates of all outgoing waves in equation (14) are to be used. Angular momentum coupling coefficients are expressed in terms of Wigner 3j and 6j symbols.

The frequency dependent polarizability $\boldsymbol{\alpha}(\omega)$ is the ratio of the induced dipole moment to the external field:

$$\boldsymbol{\alpha}(\omega) = -\frac{e}{E_0}\int Z\ \delta\rho(\mathbf{r},\omega)d\mathbf{r} \qquad (15)$$

Note that $\boldsymbol{\alpha}(\omega)$ like $\delta\rho(\mathbf{r},\omega)$ is complex. The induced density deviation (and also the corresponding induced potential) can have a phase difference with respect to that of the applied external field. Once $\boldsymbol{\alpha}(\omega)$ is determined, the photo absorption cross-section $\sigma(\omega)$ of the atom is obtained form:

$$\sigma(\omega) = \frac{4\pi\omega}{c}\operatorname{Im}\boldsymbol{\alpha}(\omega). \qquad (16)$$

Partial cross section

In order to see the connection with the IPA-model, consider the partial cross-section due to photoionization from a specific bound state $\psi_i(\mathbf{r})$ to a final continuum state $\psi_f(\mathbf{r})$.

The initial atomic state is represented as

$$\psi_i(\mathbf{r}) = \frac{U_{nl}(r)}{r} Y_L(\mathbf{r}) \qquad (17)$$

and the final continuum state with wave function **K** and energy ε as

$$\psi_f(\mathbf{r}) = 4\pi \sum_{L'} A_{l'} i^{l'} \frac{P\varepsilon l'(r)}{r} Y^*_{L'}(\mathbf{K}) Y_{L'}(\mathbf{r}) \qquad (18)$$

The complex coefficients A_l's are found by requiring $\psi_f(\mathbf{r})$ behaving asymptotically as an incident plane wave plus a spherical wave. Then the partial cross-section σ_{nl} is shown to be

$$\sigma_{nl}(\omega) = 2(2l+1)\alpha\ \eta\ \omega\sqrt{\varepsilon}\, a_B^2 \sum_{L'} \left|A_l^2\right| \langle l\ \ 100 | l'0\rangle^2 \Big| \qquad (19)$$

$$\int P_{\varepsilon l'}(r) V^{SCF}(r,\omega) U_{nl}(r) dr\Big|^2$$

where $\langle l\ \ 100|l'0\rangle$ is a Clebsch-Gordan coefficient.

In (19), V^{SCF} (r, ω) is a frequency dependent complex self-consistent potential.

3. RESULTS AND DISCUSSION

Fig.1 shows photoionization of Barium (Ba) in the photon energy range 140 – 270 eV. This energy region was selected for the present study in the context of recent experimental results [5-6] and theoretical calculations [5-6] for Barium in this energy range. In the relativistic random phase approximation (RRPA) and relativistic random phase approximation with relaxation (RRPA-R) [7] theoretical result disagreement of the experimental data suggest re-examination. So that we applied DFM which includes correlation and polarization along with relativistic effects, our present theoretical result (length form) considerable agreement in intermediate energy and give better agreement in higher energy range, but little disagreement in lower photon energy range of experimental data [7-8].

4. CONCLUSION

It is demonstrated that the time-dependent linear response method within the framework of local relativistic density functional theory can provide reliable atomic data for various atoms and ions of experimental interest.

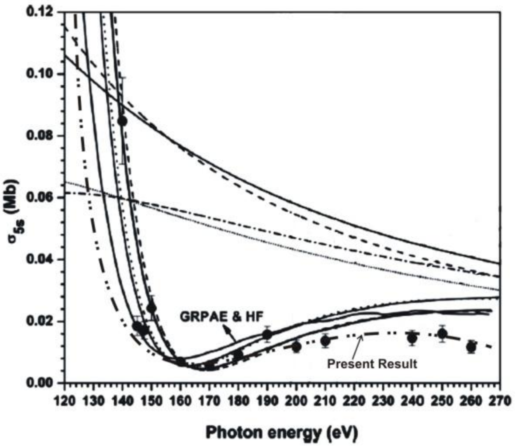

Fig. 1. photoionization of Barium (Ba),

⌶	Experimental Data : Whitfield, Wehlitz and Dolmatov [Ref.5]
·········	RRPA : Ganesan et al [Ref. 7]
– – – –	RRPA: Ganesan et al [Ref. 7]
———	GRAPE & HF : Whitfield, Wehlitz and Dolmatov [Ref.6]
– · – · ·	RRPA : Ganesan et al [Ref.7]
———	RRPA: Ganesan et al [Ref.7]
━ · · ━	DFM [2,3,4] : Present Result (Length form)

This model is particularly useful in those situations where conventional independent particle models fail to provide accurate data. The mechanism of time-dependent polarization of the atom is seen to be important in describing the observed results. As a practical point, the computer code based on the time-dependent model is fast and efficient, capable of generating a large number of data in a short time (for example , cross-sections for 10 photon energies for a medium-Z atom takes about 3 minutes of c. p. u. times on a Cray-XMP computer). The present method is capable of treating large complex atoms with high-Z for which relativistic effects are important.

REFERENCES

[1]. U. Fano and J. W. Cooper, Rev. Mod. 40, pp. 441 (1986).
[2]. M. J. Scott and E. Zaremba, Phys. Rev. A 21, pp. 12 (1980).
[3]. A. Zangwill and P. Soven, Phys. Rev. A 21, pp. 1561 (1980).
[4]. D. Liberman and A. Zangwill, Computer. Physical Communication 32, pp. 75 (1984).
[5]. S. B. Whitfield, R. Wehlitz and V. K. Dolmatov, J. Phys. B: At. Mol. Opt. Phys. 44, pp. 165002 (2011).
[6]. S. B. Whitfield, R. Wehlitz and V. K. Dolmatov, J. Phys. : Conf. Ser. 388, pp. 022008 (2012).
[7]. A. Ganesan, S. Deshmukh, G. B. Pradhan, V. Radojevic, S. T. Manson and P. C. Deshmukh, J. Phys. B: At. Mol. Opt. Phys. 46, pp. 185002 (2013).
[8]. M. Stener, P. Decleva, D. M. P. Holland and D. A. Shaw, J. Phys. B: At. Mol. Opt. Phys. 44, pp. 075203 (2011).
[9]. V. Radojevic, M. Kutzner and H. P. Kelly, Phys. Rev. A 40, pp. 727-734 (1989).
[10]. W. R. Johnson and C. D. Lin, Phys. Rev. A 20, pp. 964-977 (1979).
[11]. R. G. Parr, and W. Yang, Density-Functional Theory of Atoms and Molecules, OUP, Oxford, (1989).
[12]. N. H. March (ed.), Electron Correlation in the Solid State, ICP, London, (1999).
[13]. J. Callaway and N. H. March, Density Functional Methods: Theory and Applications, Solid State Physics, 38, pp.135 (1984).
[14]. O. Gunnarsson, M. Jonson and B. I. Lundqvist, Phys. Rev. B 20, pp. 3136 (1979).
[15]. A. Zangwill and P. Soven, Phys. Rev. Lett. 45, pp. 204 (1980).
[16]. Johnson, C. D. Lin, K. T. Cheng and C. M. Lee, Pys. Scr. 21, pp. 409 (1980).